Frontiers in Bioscience Landmark

*Front. Biosci. (Landmark Ed)* **2023**; 28(8): 160
https://doi.org/10.31083/j.fbl2808160

*Original Research*

# Rab2 and Rab6 are Implicated in Acrosome Formation during Spermatogenesis in *Eriocheir sinensis*: Based on Sperm Proteome

Chao Li[1,2], Jiao Chen[1], Shumei Mu[1,2], Han Zhang[1,2], Mingshen Guo[1,2], Yanqin Li[1,2], Zhaohui Zhang[3], Xianjiang Kang[1,2,4,*]

[1]College of Life Science, Hebei University, 071000 Baoding, Hebei, China
[2]Institute of Life Science and Green Development, Hebei University, 071000 Baoding, Hebei, China
[3]Department of Reproductive Medicine, Baoding First Central Hospital, 071000 Baoding, Hebei, China
[4]Hebei Province Innovation Center for Bioengineering and Biotechnology, Hebei University, 071000 Baoding, Hebei, China
*Correspondence: xjkang218@126.com (Xianjiang Kang)
Academic Editor: Brenda M. Alexander
Submitted: 31 January 2023 Revised: 26 March 2023 Accepted: 20 April 2023 Published: 7 August 2023

**Abstract**

**Background**: Rab proteins are GTP-dependent small proteins that function as regulators of intracellular vesicle transport, fusion, and localization. However, few studies have investigated their function in Decapoda reproduction. The *Eriocheir sinensis* sperm has no tail and the nuclei are uncondensed. With the acrosome forming the majority of the sperm mass, it provides an ideal model for studying acrosome formation. **Methods**: We firstly analyzed the sperm proteome using LC-MS/MS. To study the functions of Rab2 and Rab6, related to the Golgi apparatus, in the acrosome formation during spermatogenesis, the genes of *Rab2* and *Rab6* were cloned based on the testis transcriptome of *E.sinensis* and poly-clonal antibodies were prepared. The presence of 2 Rab proteins was confirmed in the testis and sperm by western blot. We further observed the characteristics of target 2 Rab proteins using immunofluorescence (IF). **Results**: A total of 1247 proteins including 7 Rab proteins, Rab1, Rab2, Rab5, Rab6, Rab11, Rab14, and Rab18 were identified in the sperm proteome. The IF results showed that Rab2 co-localizes with GM130, a cis-Golgi matrix protein, in the spermatagonia and spermatocytes. In the early spermatids, Rab2 and Rab6 participate in the formation of pre-acrosomal vesicles. In maturing spermatids, both Rab2 and Rab6 settle on the acrosomal membrane but present different characteristics wrapping the pre-acrosome. In the mature sperm, Rab2 localizes in the perinuclear theca surrounding the nuclei cup, while Rab6 remains on the acrosomal membrane. **Conclusions**: Our research found 7 Rab proteins based on the analysis of the sperm proteome in *E.sinensis*, and confirmed the involvement of Rab2 and Rab6 in acrosome formation. These findings provide a foundation for studying the functions of Rab proteins during spermatogenesis in Decapoda animals.

**Keywords:** *Eriocheir sinensis*; sperm proteome; LC-MS/MS; Rab2; Rab6; acrosome formation; spermatogenesis

## 1. Introduction

Rab proteins are small molecules dependent on guanosine 5'-O-(γ-thio)triphosphate (GTPs) that belong to the Ras superfamily. Over 70 human Rab proteins have been identified [1]. The major functions of Rab proteins include managing the cell inner membrane, such as vesicle transport, localization, and fusion [2]. In addition, Rab proteins are involved in the maintenance of the morphological function of mitochondria [3], the endoplasmic reticulum [4], lysosomes [5], and other membranous organelles. It has been proposed that around one-third of the Rab proteins are related to the Golgi apparatus [6]. The acrosome is a unique membranous organelle that exists in mature sperm and most organelles including the Golgi apparatus are essential for acrosome formation. Until now, 12 Rab proteins, have been found to be involved in male meiosis [7], but only Rab2 [8], Rab3 [9], Rab5 [10], Rab6 [11], Rab7 [12], and Rab27 [13] have been reported to participate in acrosome formation during spermatogenesis.

Rab2 is essential for pre-Golgi trafficking [14], while Rab6, as the most abundant Golgi-associated Rab protein, is involved in Golgi transport [15–17]. Previous studies have identified Rab2 in the acrosomal matrix of mouse sperm [18]. Bae *et al.* [19] found that Rab2 is mainly located in the midpiece of the mouse sperm and is present during spermatogenesis. Lo *et al.* [20] found Rab2 plays a significant role in protein delivery to the flagellum in human sperm. Rab6 is involved in all the stages of spermatogenesis and finally settles in the acrosomal inner membrane in the mature mouse sperm [11]. However, the roles of Rab2 and Rab6 during spermatogenesis in crustaceans remain unknown. Rab proteins have also been reported to be involved in biological processes such as endocytosis [21], autophagy [22], and organelle interactions [23]. Few studies have investigated Rab proteins in crustacea reproduction. Filling these gaps in knowledge will help to better understand the functions and mechanisms of these Rab proteins.

The sperm proteome has been reported in many mammals including humans [24], mice [25], rats [26], and dolphins [27]. The proteome of other aquatic animals including the giant grouper [28] and carp [29] has been reported, but information regarding Decapoda species like shrimp

and crab is limited. As a Decapoda animal, *E.sinensis* (Chinese mitten crab) distribute over a wide area globally. The sperm in *E.sinensis* is unique with a large acrosome surrounded by the uncondensed nuclear cup. Although *Eriocheir sinensis* sperm have no tail, the apical cap, acrosomal tubule, fibrous layer, lamellar structure, and middle layer are obvious [30]. The unique sperm characteristics of *E.sinensis* make it an ideal experimental model for studying acrosome formation.

## 2. Materials and Methods

### *2.1 Animals*

Male *E.sinensis* were purchased from Panjin, Liaoning province, China. No official approval was required for this study of the crab in China.

Balb/c female mice, used for antibody production, were purchased from Beijing Vital River Laboratory Animal Technology Co., Ltd (Beijing, China) and housed in an SPF animal house (constant temperature of 22–25 °C, relative humidity of 40–70%). Male rabbits, used for antibody production, were from Animal Experiment Center of Hebei University, and were provided food and water *ad libitum*. Experimental protocols were approved by the Institutional Animal Care and Use Committee of Hebei University. The mice and rabbits were managed per the guidelines for Animal Care and Use of Hebei University.

### *2.2 Antibodies*

GM130 (ab52649), Goat anti-Rabbit IgG H&L (Alexa Fluor® 488) secondary antibody (ab150077), goat anti-mouse IgG H&L (Alexa Fluor® 594) secondary antibody (ab150116) were purchased from Abcam (Cambridge, MA, USA). Horseradish peroxidase (HRP)-conjugated goat anti-rabbit and goat anti-mouse antibodies were purchased from Beijing Solarbio Science & Technology Co., Ltd. (Beijing, China).

### *2.3 SDS-PAGE of Sperm Protein*

Seminal vesicles and accessory glands were obtained from mature male crabs frozen on ice for 15 min before dissection. The spilled spermatophores from seminal vesicles were washed twice using precooled (4 °C) $Ca^{2+}$-free artificial seawater (FASW)-(475 mM NaCl, 12 mM KCl, 30 mM $MgCl_2 \cdot 6H_2O$, 20 mM Tris, pH 8.2). The liquid was discarded using a straw after spermatophores precipitated on ice. Proteins from the accessory gland were collected after homogenization and centrifugation at 4 °C, 12,000 g, and 5 min to digest the spermatophores. The crude sperm were released within 15 min; all the components were transferred to a centrifuge tube. The supernatant containing released sperm was collected after centrifugation at 4 °C, 200 g, 10 min. After washing 3 times with FASW and centrifugation at 4 °C, 850 g, 10 min, the pure sperm were obtained.

Proteins from crab sperm were extracted on ice using 8 M urea lysate (8 M urea, 3 µM total sialic acid, and 50 mM nicotinamide). Phenylmethylsulfonyl fluoride (PMSF) was added before use (final concentration 1 mM). 1 mL of precooled urea lysate was added to 50 mg sperm and incubated for 5 min on ice, then ultrasonication was conducted at 30% power, 2 s on, 3 s off, for 2 min using an ultrasonic processor (Scientz, Ningbo, China). Then, the proteins were obtained via centrifugation at 4 °C, 12,000 g for 20 min, with the sperm proteins ultimately collected from the supernatant. Proteins were stored at –80 °C after measuring their concentration with a BCA Kit ( P0012S, Beyotime, Beijing, China).

The proteins were mixed with loading buffer (SL1170-1 mL, Coolaber, Beijing, China) and denatured at 100 °C for 5 min. A total of 20 µg of each sample was separated in 15% polyacrylamide gels with 5% stacking gel for SDS-PAGE and the gels were stained for protein with Coomassie Brilliant Blue R-250 (CBB).

### *2.4 LC-MS/MS*

LC-MS/MS analyses of sperm proteins were conducted at Jingjie Company (Hangzhou, China). We summarized the steps as follows. The proteins were separated using 10% polyacrylamide gels and SDS-PAGE was finished when the protein migrated 1 cm from the stacking gel. After staining by CBB and then a destaining buffer, the gels were cut into small granules on clean glass. For digestion, the protein solution was reduced with 5 mM dithiothreitol for 30 min at 56 °C and alkylated with 11 mM iodoacetamide for 30 min at room temperature in darkness. The protein sample was then diluted by adding 100 mM triethylammonium bicarbonate (TEAB) to a urea concentration less than 2 M. Finally, trypsin was added at 1:50 trypsin-to-protein mass ratio for the first digestion overnight and 1:100 trypsin-to-protein mass ratio for a second 4 h-digestion. Finally, the peptides were desalted by C18 solid phase extraction (SPE) column.

The desalted and lyophilized peptides were reconstituted with 0.1% formic acid (FA) which contains 2% acetonitrile and loaded onto a home-made reversed-phase analytical column (25-cm length, 75/100 µm i.d.). Peptides were separated with a gradient from 6% to 24% solvent B (0.1% formic acid in acetonitrile) over 70 min, 24% to 35% in 14 min, and climbing to 80% in 3 min then holding at 80% for the last 3 min, all at a constant flow rate of 450 nL/min on a nanoElute Ultra-high-pressure liquid chromatography (UHPLC) system (Bruker Daltonics, Bremen, Germany).

The peptides were subjected to a capillary source followed by the timsTOF Pro (Bruker Daltonics) mass spectrometry. The electrospray voltage applied was 1.60 kV. Precursors and fragments were analyzed at the TOF detector, with an MS/MS scan range from 100 to 1700 m/z. The timsTOF Pro was operated in parallel accumulation serial fragmentation (PASEF) mode. Precursors with charge state 0 to 5 were selected for fragmentation, and 10 PASEF-MS/MS scans were acquired per cycle.

*2.5 Database Search*

The resulting MS/MS data were processed using the MaxQuant search engine (v.1.6.15.0, http://www.maxquant.org/). Tandem mass spectra were searched against the transcriptome of testis and sperm connected with downloaded data that reported data in the SwissProt database on *E.sinensis*. Reverse decoy databases were used to guarantee the correction rate. Trypsin/P was specified as the cleavage enzyme allowing up to 2 missing cleavages. The mass tolerance for precursor ions was set as 20 ppm in the first search and 5 ppm in the main search, and the mass tolerance for fragment ions was set as 0.02 Da. Carbamidomethyl on Cys was specified as a fixed modification, and acetylation on protein N-terminal and oxidation on Met were specified as variable modifications. The false discovery rate (FDR) was adjusted to $<1\%$.

*2.6 GO Annotation*

Gene Ontology (GO) annotation proteome was derived from the UniProt-GOA database (http://www.ebi.ac.uk/GOA/). Firstly, the identified protein ID was converted to UniProt ID and then mapped to GO IDs by the protein ID. If some identified proteins were not annotated by the UniProt-GOA database, the eggNOG-mapper (v2.0 https://github.com/eggnogdb/eggnog-mapper) was used to annotate the protein's GO function based on the protein sequence alignment method. Then proteins were classified by GO annotation based on three categories: biological process, cellular component, and molecular function.

*2.7 Subcellular Localization*

The cells of eukaryotic organisms are elaborately subdivided into functionally distinct membrane-bound compartments. Some major constituents of eukaryotic cells are the extracellular space, cytoplasm, nucleus, mitochondria, Golgi apparatus, endoplasmic reticulum, peroxisome, vacuoles, cytoskeleton, nucleoplasm, nucleolus, nuclear matrix and ribosomes. There, we used wolfpsort a subcellular localization prediction software to predict subcellular localization.

*2.8 Rab2 and Rab6 Cloning*

Testes from male crabs were dissected on ice and washed twice with $Ca^{2+}$-free artificial seawater ($Ca^{2+}$-FASW; containing 475 mM NaCl, 12 mM KCl, 30 mM $MgCl_2$, 20 mM Tris, pH 8.2). RNA was extracted with Trizol and then reverse-transcribed into cDNA using a kit (RR047A, Takara, Beijing, China).

Primers of *Rab2* (GenBank accession No. LOC126998668) and *Rab6* (GenBank accession No. LOC127008679) were designed in our laboratory; the sequences were as follows: *Rab2*. F1, 5′-ATGTCCTACGCCTATTTATTCAA-3′, and R1, 5′-CTTGTTTCCAATCAGCATGAT-3′. *Rab6*. F2, 5′-ACAGTTCGACTGCAGCTCT-3′, R2, 5′-ACACCCACCATCGGCTGTC-3′. Primers were synthesized by Songon Biotech (Shanghai, China). The PCR steps were as follows: Rab2: 94 °C for 30 s, 62 °C for 30 s, 72 °C for 40 s, and 30 cycles. 72 °C was kept for 10 min for the last cycle. Rab6: 94 °C for 30 s, 58 °C for 30 s, 72 °C for 40 s, and 30 cycles. 72 °C was kept for 10 min for the last cycle. 1.0% agarose gels were used to check the PCR products, *Rab2* was obtained at 360 bp of and *Rab6* at 450 bp, as expected. To further verify the accuracy, the PCR products were sequenced by the Sanggon Company (Shanghai, China) after recovery with an Agarose Gel DNA Recovery kit (Beijing Biotechnology Co. Ltd., Beijing, China).

*2.9 Expression and Purification of Rab2 and Rab6*

Pet-19T-Rab2 and Pet-19T-Rab6 were prepared with a Pet-19T cloning vector (Takara). After sequencing by the Sanggon Company (Shanghai, China), both recombined vectors were transformed into BL21 for multiplication. Stocks were stored at –80 °C. Rab2 primers were designed with BamH I (identified in the sequence by underlining) at the forward primer 5′-CGCGGATCCATGTCCTACGCCTATTTATTCAA-3′ and XhoI (underlined) at the reverse primer 5′-ACGTCACTCGAGCTTGTTTCCAATCAGCATGAT-3′. Rab6 primers were designed with NdeI (underlined) at the forward primer. 5′-ACGCGCCATATGACAGTTCGACTGCAGCTCT-3′, and XhoI (underlined) at the reverse primer 5′-ACGTCACTCGAGACACCCACCATCGGCTGTC-3′.

Pet-19T-Rab2 and Pet-19T-Rab6 were used as the template using the above primers for PCR. The products were digested with BamH I and XhoI for Rab2, and NdeI and XhoI for Rab6. Rab2 was incorporated in the Pet-28b vector while Rab6 was incorporated in the Pet-21b vector. Recombinant clones for expression are named Pet-28b-Rab2 and Pet-21b-Rab6. All were validated via sequencing by the Sangon Company (Shanghai, China).

The recombinant plasmid Pet-28b-Rab2 was transformed into electrocompetent BL-21 and selected with Luria–Bertani (LB) plates containing kanamycin (10 μg/mL). The remaining BL-21 was expanded at 37 °C for 4 h with shaking at 180 RPM with a final concentration of 0.2 mmol/L of isopropyl $\beta$-D thiogalactoside (IPTG). The culturing was ended when the OD value was read as 0.4–0.6, then centrifuged (4 °C, 1000 g, 10 min) to collect the pellets. A fragmentation buffer (100 mM $NaH_2PO_4$, 10 mM Tris–HCl, 8 M urea) was added to the strains, then fragmented using ultrasonic shearing (Ningbo, Scientz D) on ice (60% intensity, 5 s, 10 s interval, 6 min). The suspensions were centrifuged (4 °C, 12,000 g, 30 min) in 50 mL tubes to separate the supernatant and precipitant. The supernatant was purified using a nickel column and eluted with buffer (25 mM Tris 25 mL, 15 mM NaCl, 3% Midazole, pH 8.0) to collect the target protein. We used 15% SDS-PAGE to verify the purified Rab2 and Rab6.

*2.10 Preparation of Rab2 and Rab6 Polyclonal Antibodies*

Balb/c female mice aged 6 weeks were habituated for 1 week. 50 µg Rab2 polypeptide antigen mixed with 50 µg Freund's complete adjuvant (lot number: F5881; Sigma, St. Louis, MO, USA) was injected into the back of the mice for the first immunization. 10 days later, a second immunization was performed by emulsifying half of the antigen polypeptide with an equal volume of Freund's incomplete adjuvant (lot number: F5506; Sigma, St. Louis, MO, USA) using intraperitoneal injection. The health status of each animal was observed after each injection. The last two immunizations were prepared as the second injection and injected once weekly. Three days after the last immunization, blood was collected from the eye socket with a glass capillary and the serum was extracted. Anti-Rab2 serum was stored at –80 °C.

Rab6 polyclonal antibodies were prepared similarly, but by using rabbits instead of mice for more anti-serum. Two male New Zealand White rabbits ($2 \pm 0.3$ kg) were housed in 2 pens ($1.0 \times 0.7$ $m^2$) individually at the Animal Experiment Center of Hebei University. A week later, each rabbit was immunized with 0.5 mg of the Rab6 polypeptide mixed with Freund's Complete Adjuvant (lot number: F5881; Sigma, St. Louis, MO, USA) via multi-point subcutaneous injection. The last 3 immunization were performed every 10 days using Freund's Incomplete Adjuvant (lot number: F5506; Sigma, St. Louis, MO, USA), delivered via intraperitoneal injection. Three days after the last immunization, blood was collected from the ear vein and serum was separated. Anti-Rab6 serum was stored at –80 °C.

*2.11 Enzyme-Linked Immunosorbent Assay (ELISA)*

Anti-Rab2 antiserum was collected after centrifugation (12,000 g, 10 min, 4 °C) and quantified by indirect ELISA using the above purified Rab2 as the antigens. The optimal dilution (2 µg/mL) of recombinant protein was used to coat the 96-well plate, and the samples were blocked with 100 µL 10% BSA diluted in washing buffer (0.0015 M $KH_2PO4$, 0.008 M $Na_2HPO_4 \cdot 12\ H_2O$, 0.14 M NaCl, 0.003 M KCl, 0.05% v/V Tween-20) for 2 h at room temperature. The primary antibody anti-Rab2 serum and preimmune serum were diluted (1:100 to 1:102,400). A total of 100 µL goat to mouse IgG with conjugated HRP (dilution 1:1000, Solarbio, Beijing, China) was added and incubated at 37 °C for 1 h. After washing three times the reaction termination liquid (10% v/V $H_2SO_4$) was added. Anti-Rab6 antiserum was similarly detected. The difference is that the second polyclonal goat anti-rabbit IgG with conjugated HRP (dilution 1:1000, Solarbio) was used. Finally, the titer of the polyclonal antibody was measured and analyzed based on a 450 nm absorbance value using a multifunctional microplate reader (Molecular Devices, Shanghai, China).

*2.12 Western Blot Analysis*

Western Blot was used to detect the specificity of Rab2 and Rab6 polyclonal antibodies. Proteins from crab testes were extracted on ice using a radioimmunoprecipitation assay (RIPA) lysis buffer (Beyotime, China, cat#P0013B) with 10 µL PMSF to a final concentration of 1 mM. A total of 20 µg of the sample was loaded using 15% sodium dodecyl sulfate-polyacrylamide separation gel electrophoresis (SDS-PAGE) for detection. The gel was cut between 10–25 kD and transferred to a polyvinylidene fluoride membrane (PVDF) membrane. The membranes were incubated with Rab2 polyclonal antibodies overnight at 4 °C after blocking with 5% skim milk in TBST (tris buffered saline and 0.1% Tween-20) for 2 h at room temperature. Then, HRP-conjugated goat anti-mouse IgG (dilution 1:1000, Solarbio) after washing 3 times with TBST. Finally, enhanced chemiluminescence (ECL) reagent kit (Solarbio, China, cat#PE0010) was used for detection. Rab6 or GM130 (ab52649) was detected using the same method, the difference is that Rab6 or GM130 antibodies were used instead of Rab2, and the secondary antibodies for HRP-conjugated goat anti-rabbit IgG (dilution 1:1000, Solarbio) were used for detection. $\beta$-actin was used as the loading control for the western blot. All results were acquired and analyzed with Image Lab software (v.4.1, Bio-Rad, Hercules, CA, USA). Image J software (v.13, LOCI, University of Wisconsin, Madison, WI, USA) was used for the relative protein quantification analysis.

*2.13 Immunofluorescence*

To observe the colocalization of Rab2 and GM130, testes from male crabs were fixed with 4% paraformaldehyde overnight at 4 °C and dehydrated using 30% (w/w) sucrose in 0.1 M PBS, pH 7.4. Frozen sections were permeabilized with 0.5% Triton X-100 at room temperature for 10 min, and blocked with 5% BSA, 10% goat serum, and 0.3 M glycine for 1 h at RT after 3 washes with PBS. Anti-Rab2 antiserum (dilution 1:500) along with GM130 (dilution 1:200, Abcam) were incubated for co-staining overnight at 4 °C. After washing 3 times for 10 min, the secondary antibodies of goat anti-rabbit Alexa Fluor® 488 (1:200, Abcam) and goat anti-mouse Alexa Fluor® 594 secondary antibodies (dilution 1:200, Abcam) were added and incubated at RT in the dark for 1 h at room temperature. After washing 2 times for 5 min with PBS, 6-diamidino-2-phenylindole (DAPI) was used for nuclear staining for 5 min following the last washing. Control sections were incubated with non-immune goat serum (Solarbio, China, cat#SL038) in place of primary antibodies under the same condition described above.

To observe the characteristics of Rab2 during different periods of spermatids, only Rab2 poly-antibodies were used (1:500) and goat anti-mouse Alexa Fluor® 594 secondary antibodies (dilution 1:200, Abcam) were incubated. Rab6 detection was conducted using the method described

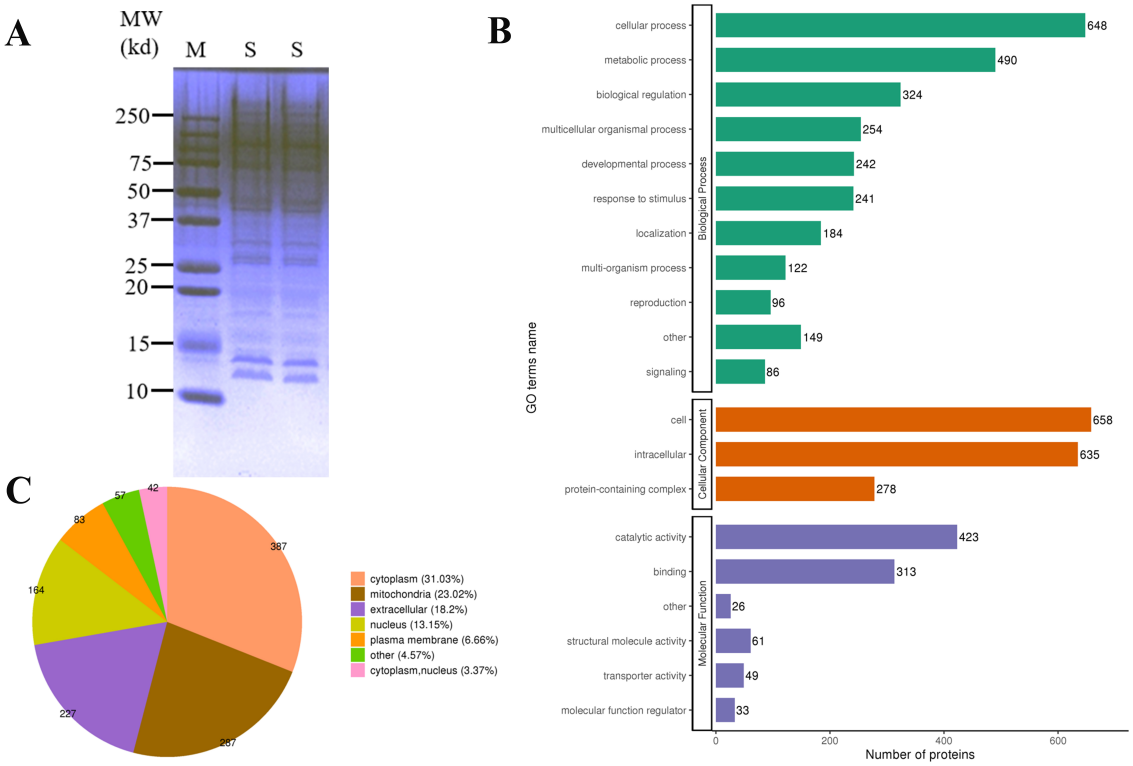


**Fig. 1. Analysis of sperm proteins.** (A) SDS-PAGE of mature sperm protein in *E.sinensis*. (B) GO annotations of the 1247 identified proteins from the proteome database: biological process, cellular component, and molecular function. (C) Subcelluar localization of the sperm proteome. Pie chart of the subcellular localization of sperm proteins predicted by wolfpsort annotation.

above. The difference is that anti-Rab6 antiserum was used (1:400) and the secondary antibodies of Alexa Fluor 488-conjugated goat anti-rabbit (dilution 1:200) were incubated at RT after washing. Both control sections were incubated without a primary antibody.

All the stained sections were mounted on slides using an anti-fade mounting medium (Southern Biotech, Cat#.0100–01). Images were acquired using an Olympus FV1000-IX81 laser scanning confocal microscope (Olympus, Tokyo, Japan).

## 3. Results

### *3.1 SDS-PAGE*

The SDS-PAGE result of sperm proteins showed a total of 23 detectable bands (Fig. 1A). Rab proteins represent 21–25 kD and the histones are under 15 kD.

### *3.2 Sperm Proteome*

LC-MS/MS was conducted to identify the sperm proteome. Raw data produced by the timsTOF Pro (Bruker Daltonics) mass spectrometry were subsequently searched by using the MaxQuant search engine (v.1.6.15.0). Tandem mass spectra were searched with the transcriptome of testis and sperm in *E.sinensis* connected with SwissProt database. A total of 26,430 peptides corresponding to 1247 proteins were identified (**Supplementary Table 1**). As expected, the major proteins fell under either catalytic activity or binding functions. A wide range of protein classes was identified with hydrolase, oxidoreductase, nucleic acid binding, transferase, cytoskeleton protein, and enzyme modulator being the most common. The results could be divided into the biological process (BP), cell component (CC), and molecular function (MF) categories (Fig. 1B).

Importantly, all previously identified histone proteins including H1, H2A, H2B, H3, and H4 were detected [31–34]. Further cell component association analysis showed that the sperm proteome contains proteins from different organelles (Fig. 1C), such as mitochondria (287), endoplasmic reticulum (18), and Golgi apparatus (2) (**Supplementary Table 2**). 6 cathepsin proteins including A, B, C, D, F, and L were detected in the mature sperm. In addition, 7 types of Rab proteins, including Rab1, Rab2, Rab5, Rab6, Rab11, Rab14, and Rab18 were found.

### *3.3 Detection and Sequencing of Rab2 and Rab6*

RNA quality was assessed with 1% agarose gel electrophoresis (Fig. 2A). A band was seen at approximately 360 bp as expected for *Rab2* (Fig. 2B) while *Rab6* was seen at 450 bp (Fig. 2C). *Rab2* was cleaved from Pet-19T-Rab2 with BamH I and XhoI and sequenced after gel-purification; *Rab6* was cleaved using NdeI and XhoI from Pet-19T-Rab6 and sequenced. The results of these analyses validated our *Rab2* and *Rab6* preparation.

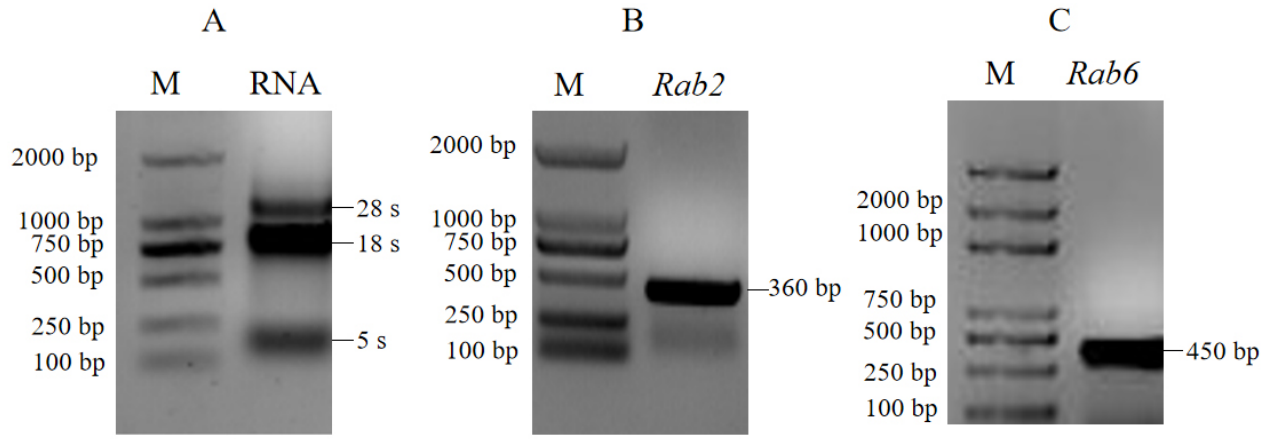


**Fig. 2. Detection of total RNA, *Rab2*, and *Rab6*.** (A) 3 bands of total RNA from the testis in *E.sinensis* in the gel. (B) A band around 360 bp represents *Rab2*. (C) A band around 450 bp represents *Rab6*. M, Marker.

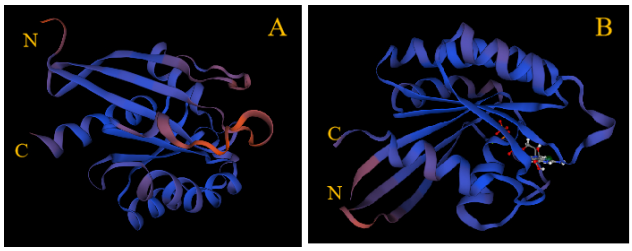


**Fig. 3. The spatial structures of Rab2 (A) and Rab6 (B) domains predicted by SWISS-MODEL.** Both structures contain typical central six-strand $\beta$-sheets flanked by several $\alpha$-helices.

*Rab2* sequencing results are the same as part of the gene *Rab2* sequence (total 642 nucleotides). The primers are underlined and the sequence of *Rab2* (360 nucleotides) for PCR are denoted in bold.

**ATGTCCTACGCCTATTTATTCAAGTACATCA
TCATCGGAGACACTGGTGTGGGGAAGTCATGT
CTCCTGCTACAGTTCACGGACAAGAGGTTCCA
GCCAGTGCACGACCTCACCATCGGGGTGGAGT
TTGGTGCCCGCATGATCACCATTGACAACAAG
CAGATCAAGCTTCAGATTTGGGACACAGCTGG
CCAAGAGGCATTCAGGTCCATCACAAGGTCAT
ACTACCGTGGAGCAGCCGGCGCCCTTCTGGTC
TATGACATCACCAGGCGGGAAACCTTCAACCA
CCTCACGCAGTGGCTAGAAGATGCTCGCCAGC
ACTCCAACTCCAACATGGTCATCATGCTGATTG
GAAACAAG**AGTGATCTTGACTCACGGCGAGAGG
TAAAGCGAGAAGAGGGCGAAGCCTTTGCGCGGG
AGCACGGGCTGGTGTTCATGGAGACCTCCGCCAA
GACCGCCGCCAACGTAGAGGAAGCTTTCATCAAC
ACTGCCAGGGAAATCTACGAGAAGATCCAGGAGG
GGGTGTTTGACGTCCACAATGAGGCTAACGGCAT
CAAGATTGGGCCCCAGCACTCCCCCGGAGGAGCC
GGCCTCACCAACAACCAGGGAGCCGCTGGCGGTC
AAGGCGGCGGCTGCTGTTAA

*Rab2* coding proteins sequence. The protein sequence of Rab2 (total 213 amino acids) is shown as follows and the selected immunogenic protein sequence of Rab2 (120 amino acids) is denoted in bold.

**MSYAYLFKYIIIGDTGVGKSCLLLQFTDKRFQ
PVHDLTIGVEFGARMITIDNKQIKLQIWDTAGQE
AFRSITRSYYRGAAGALLVYDITRRETFNHLTQW
LEDARQHSNSNMVIMLIGNK**SDLDSRREVKREEG
EAFAREHGLVFMETSAKTAANVEEAFINTAREIYEK
IQEGVFDVHNEANGIKIGPQHSPGGAGLTNNQGAA
GGQGGGCC

*Rab6* sequencing results are the same as part of the gene *Rab6* sequence (total of 639 nucleotides). The primers are underlined and the sequence of *Rab6* (total 450 nucleotides) for PCR are denoted in bold.

ATGTCCATGTCGGGCGAATTTGGGAACCCGCT
CCGGAAATTCAAGCTGGTCTTTCTGGGCGAGCAAA
GCGTCGGAAAGACCTCGCTGATAACAAGGTTTATG
TACGACTCCTTTGACAACACATACCAGGCAACGAT
TGGCATAGACTTCCTCTCCAAAACAATGTACCTCG
AGGATAGA**ACAGTTCGACTGCAGCTCTGGGACA
CGGCCGGCCAGGAGAGGTTCCGTAGCCTCATC
CCATCCTATATCCGAGACTCGACTGTCGCTGTG
GTTGTGTACGACATTACCAATGCCAATTCTTTC
CACCAAACTTCTAAGTGGATAGACGATGTGAGG
ACTGAGCGAGGCAGCGACGTAATTATCATGCTG
GTTGGAAATAAGACTGATCTTTCGGACAAGAGA
CAGGTTTCCACGGAGGAGGGCGAGCGCAAGGC
CAAGGAACTCAACGTGATGTTCATTGAGACGAG
TGCAAAGGCAGGATACAATGTGAAACAGCTCTT
CCGAAGGGTGGCCGCCGCCCTACCCGGTATGG
AGTCCAATCCTGAGAAGGGCAAGGTTGACATG
ACCGAAGTTGTCCTGAGGGACTCAGACAACAC
TGCAGAGATTGGGCG**GACAGCCGATGGTGGGT
GT**GCTTGCTAG

*Rab6* coding proteins sequence. The protein sequence of Rab6 is shown as follows (total 212 amino acids) and

the selected immunogenic protein sequence of Rab6 (150 amino acids) is denoted in bold.

MSMSGEFGNPLRKFKLVFLGEQSVGKTSLITRF MYDSFDNTYQATIGIDFLSKTMYLEDR**TVRLQLWD TAGQERFRSLIPSYIRDSTVAVVVYDITNANSFHQT SKWIDDVRTERGSDVIIMLVGNKTDLSDKRQVST EEGERKAKELNVMFIETSAKAGYNVKQLFRRVA AALPGMESNPEKGKVDMTEVVLRDSDNTAEIGR TADGGC**AC

The structures of Rab2 and Rab6 domains predicted by SWISS-MODEL showed that both two Rab proteins contain β-sheets flanked by α-helices (Fig. 3).

### *3.4 Expression of Rab2 and Rab6*

The results of SDS-PAGE showed that Rab2 and Rab6 were purified as expected. A band at 15 kD represents purified Rab2 and a band at 17 kD of Rab6 after Ni column purification (Fig. 4).

### *3.5 Western Blot Analysis*

Quantification of Rab2 and Rab6 in the antisera using ELISA confirmed that both poly-antibodies were ready for the following experiments. Proteins extracted from the testes and sperm of *E.sinensis* were subjected to western blot, and the results showed a band at 22 kd for Rab2 (Fig. 5A) and a band at 26 kd for Rab6 (Fig. 5C), confirming our preparation. A band is shown at 130 kd for GM130 (Fig. 5B), validating this GM130 antibody as suitable for our research (Fig. 5D). Quantification by Image J showed that the expression of Rab2, Rab6 and GM130 in the testes was higher than in sperm (Fig. 5E–G).

### *3.6 Observation of Spermatogenesis*

In the crab testis, different stages of germ cells can be recognized according to the unique characteristics of their DAPI-stained nuclei (Fig. 6). Spermatogonia has the largest nuclei with fewer chromatin clumps compared with spermatocytes. At the spermatid stage, the chromatin becomes dense and the clumps disappear. Early spermatids have round donut-like nuclei. Middle spermatids have crescent-shaped nuclei that wrap the proacrosome. Late spermatids have cup-like nuclei that hold the acrosome. The spermatozoa in seminal vesicles have a nuclear annulus resembling a ring when observed from above.

### *3.7 Immunofluorescence*

#### 3.7.1 Rab2 Co-Localized with GM130 around the Nuclei in Spermatogonia and Spermatocytes

We found that Rab2 (red) and GM130 (green) were colocalized next to the nuclei (blue) as expected in both spermatogonia and spermatocytes (Fig. 7). The nuclei are round in the spermatogonia and spermatocytes. The nuclei in spermatogonia are larger and their chromatin is looser compared with spermatocytes, which show chromatin clumps that are randomly distributed in the nuclei. No signals could be observed in the negative control group.

#### 3.7.2 Rab2 Dynamics during Acrosome Formation

In the early spermatids, Rab2 (red) signals are mainly located at one side of the cell around the nuclei (Fig. 8). The chromatin becomes dense with a central cavern. Rab2 was transferred to the pre-acrosomal vacuoles (PV) in the middle spermatids. At this stage, Rab2 wraps the PV like a long coat with a thickening at the waist compared with the head. The nuclei transform to a crescent shape with a small central aperture. In the late spermatids, the nuclei turn into a ring that wraps the acrosome while Rab2 surrounded the nuclei. In the mature sperm, Rab2 remains surrounding the nuclei. No positive signals were observed in the negative controls.

#### 3.7.3 Rab6 Dynamics during Spermatogenesis and Acrosome Formation

Rab6 settles at one side adjacent to the nuclei in the cytoplasm in spermatogonia and spermatocytes (Fig. 9). In the early spermatids, Rab6 gathers at one side of the cell near the nuclei which indicated that it may participate in the formation of pre-acrosomal vacuoles. These signals transferred to the pre-acrosomal membrane in the middle spermatids, and finally settle on the acrosomal tubule and acrosomal membrane in the mature sperm.

## 4. Discussion

The sperm proteome has been reported among mammals, including human [24], mouse [25], rat [26], pig [35], bovine [36], and koala [37]. The proteomic analysis of spermatozoa in several species of aquatic animals has been reported, such as the giant grouper [27], bottlenose dolphin [28], and carp [29]. However, few have focused on Decapoda animals. In this study, we identified 1247 sperm proteins; as in other species, most were structure proteins, energy metabolism related proteins, cytoskeletal proteins, and enzymes. In the present study, there was a greater quantity of identified sperm proteins compared with other aquatic animals such as the bottlenose dolphin (419) [28] and carp (348) [29], but lower than mammals such as humans (4675) [38] and pigs (1723) [35]. The nuclei in *E.sinensis* is uncondensed and it was thought to be related to the types of histones; we also confirmed that all 5 histones exist in the sperm proteome, which is consistent with our previous findings [31–34]. Similar to the mouse and human sperm proteome [24,25], the sperm proteome in *E.sinensis* contains many mitochondrial proteins. These results indicate that mitochondria are involved in spermatogensis; more studies are needed to further characterise the mitochondria during acrosome formation.

Rab proteins belong to the Ras superfamily which has GTP-hydrolysis activity. Most are involved in vesicle transport between different membranes including organelles and the cell membrane [1]. The acrosome, as a membranous organelle, originates from vesicles related to the Golgi, which highlights the importance of Rab proteins during acrosome formation. In our study, 7 Rab proteins

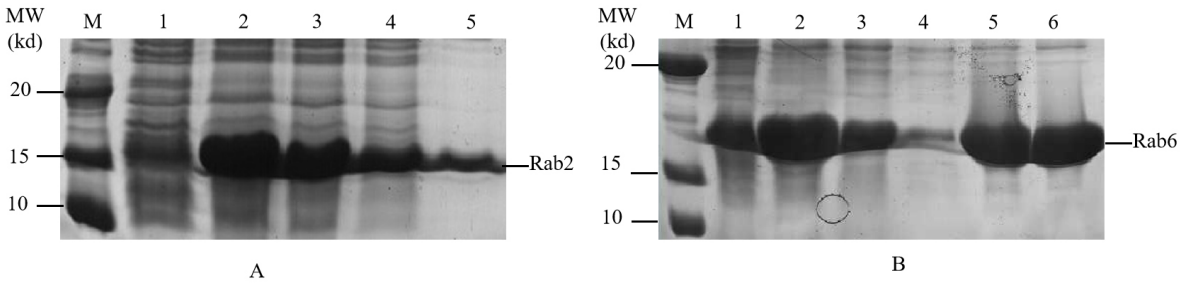


**Fig. 4. Results of Rab2 and Rab6 purification.** (A) purification of Rab2; (B) purification of Rab6. M, Marker; 1, proteins from BL-21; 2, proteins in suspension; 3, collected proteins after Ni column; 4, eluted proteins; 5,6, proteins after purification.

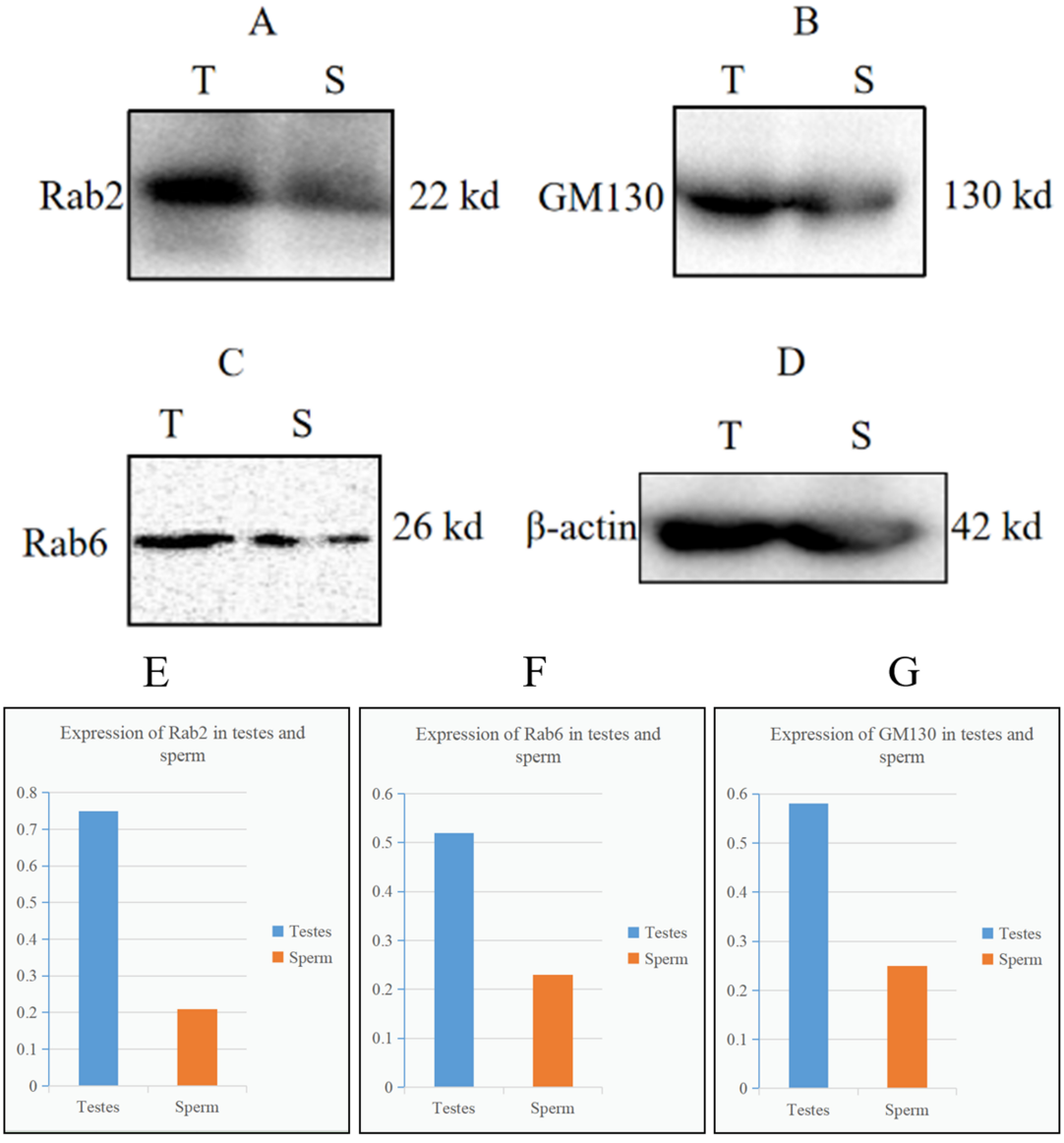


**Fig. 5. Western blot analysis using Rab2, Rab6, and GM130 antibodies of *E.sinensis* testes and sperm proteins.** A band at 22 kD represents Rab2 (A), a band at 130 kD represents GM130 (B), and a band at 26 kD represents Rab6 (C). $\beta$-actin was used as the loading control for the western blot, represented by a band at 42 kD (D). Expression of Rab2, Rab6, and GM130 in the testes was higher than in sperm (E–G). M, Marker; T, testes proteins; S, sperm proteins.

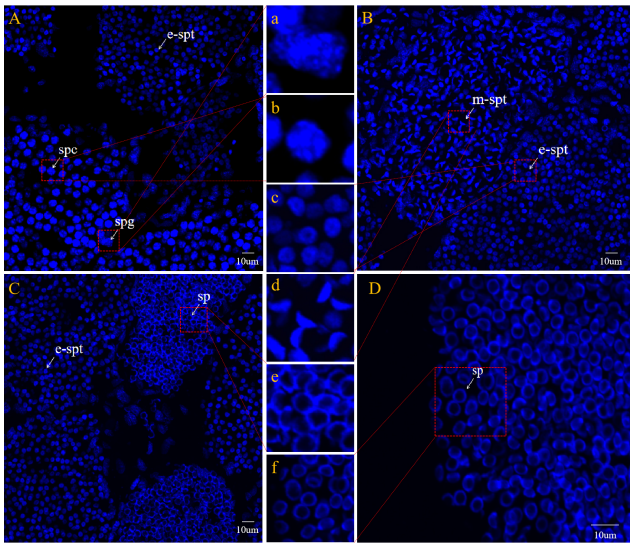


**Fig. 6. Different stages of germ cells of the testis in *E.sinens* stained by DAPI.** The nuclei in spermatogonia are round with fewer chromatin clumps and the chromatin is looser compared with spermatocytes (A). Early spermatids have condensed donut-like chromatin (A–C). Sperm have cup-like nuclei (D). Middle spermatids have crescent nuclei settled at one side of the cell. The nuclei in the late spermatids are a little thicker than in mature sperm, and the radial arms emerge till spermatozoa. SPG (a): spermatogonia; SPC (b): spermatocyte, eSPT (c): early spermatid, mSPT (d): middle spermatid, lSPT (e): late spermatid, SP (f): spermatozoa. The scale bar represents 10 μm.

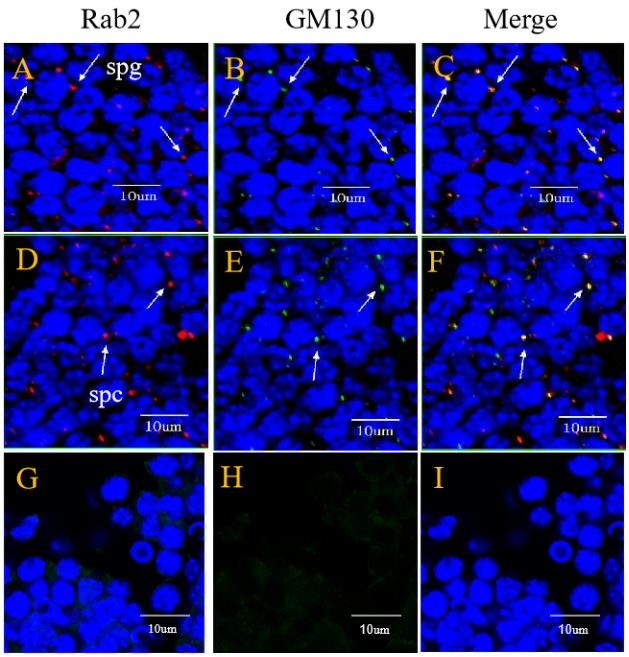


**Fig. 7. Rab2 (red) is co-localized with GM130 (green) in the spermatogonia and spermatocytes during spermatogenesis.** The size of the nuclei in spermatogonia is larger (8–10 μm) compared with spermatocytes (5–9 μm), but the chromatin is looser. Rab2 together with GM130 is located in the Golgi apparatus adjacent to the nuclei, both in spermatogonia (A–C) and spermatocytes (D–F). In the negative controls, no positive signals were observed (G–I). spg, spermatogonium; spc, spermatocyte.

were identified, including Rab1, Rab2, Rab5, Rab6, Rab11, Rab14, and Rab18. Baker *et al*. [26] found 858 proteins in the mouse sperm proteome, and the Rab family including Rab2, Rab5, Rab8, Rab11, Rab14 and Rab 22 (but not Rab 6), as a second family of proteins that are highly represented in the sperm. Chauvin further found 2850 proteins using the deep mouse epididymal sperm proteome [25] and increased the number of identified Rab proteins to 23. Published data underline the important role of Rab proteins. It has been reported that Rab2, Rab3, Rab5, Rab6, Rab7, and Rab27 are involved in acrosome formation during spermatogenesis of various species [8–13]. We identified Rab2 and Rab6 in the sperm proteome in this study; these results are analogous to what is seen in mammals [8,11,18]. We did not detect Rab3, but Rab3 is present in the acrosomal region of mouse, rat and human sperm [9,39]. Other Rab proteins, related to male fertility, are involved in sperm motility and capacitation [19,40]; more research is needed to fully identify the functions of Rab proteins in germ cells in Decapoda animals.

The involvement of Rab2 and Rab6 in spermatogenesis has been described in mice and cattle [41,42]. Rab2 has been ascribed to the formation of pre-acrosomal vesicles in the Golgi and cap phases of spermiogenesis and eventually forms the perinuclear theca in bovine sperm [8]. Similarly, in our study, Rab2 locates on the membrane of pre-acrosomal membrane in the early and middle spermatids. In the mature sperm, Rab2 transfer to the perinuclear theca around the nuclei, which indicates the importance of Rab2 for sperm maturation. It has been confirmed that Rab2 is important for the maturation of Golgi precursors [43]. We found Rab2 co-localized with GM130 in spermatogonia and spermatocytes, confirming that Rab2 is on the Golgi apparatus, which parallels with the somatic cells. It has been found that Rab2, generated from the Golgi apparatus, is essential to autophagy [44,45]. Autophagy is essential for spermatogensis, more efforts are necessary for confirming whether Rab2 is related to autophagy during spermatogenesis in *E.sinensis*.

Rab6, as the most abundant Golgi Rab protein, was found to be essential for shaping the Golgi apparatus in yeast [46]. In germ cells, Da Costa [11] found that Rab6 together with Vps13b are located at the Golgi apparatus of all spermatogenic cells, and finally settle down on the acrosomal membrane connected by Vps13b in the spermatozoa. Though the sperm of *E.sinensis* are unique, we found that Rab6 is involved in pre-acrosome granule formation in the early spermatids, and gradually transfers to the acrosomal membrane in the middle spermatids. In the mature sperm, Rab6 exists on the central tubule alongside the acrosomal

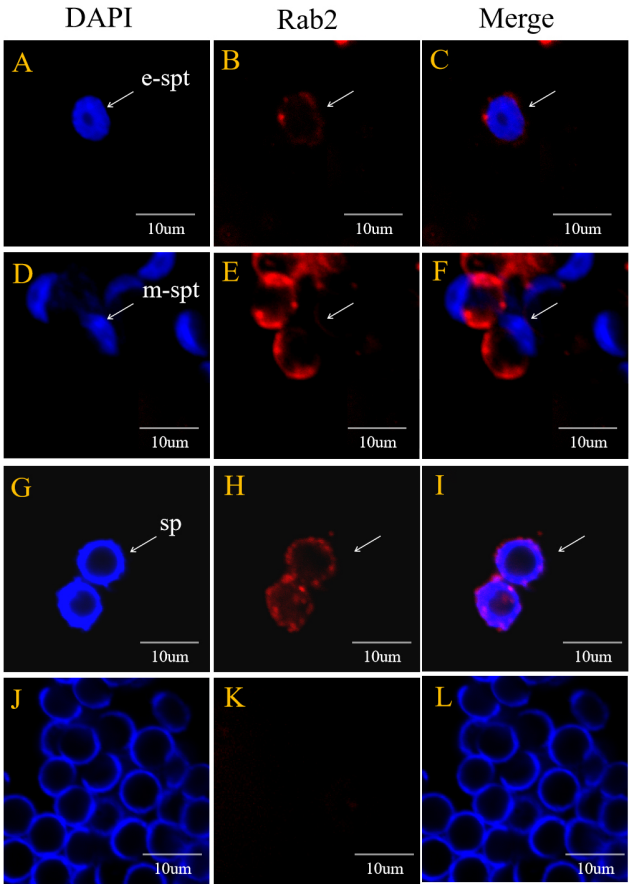


**Fig. 8. Rab2 (red) was involved in the formation of pro-acrosomal vacuoles (PV) in spermatids.** In the early spermatids, Rab2 localized at one site adjacent to the dense nuclei (A–C). In the middle spermatids, the nuclei transformed into a crescent shape, Rab2 wrapped the PV and was thicker at the waist and thinner in the head (D–F). In the mature sperm, Rab2 surrounds the ring nuclei (G–I). In the negative controls, no positive signals were observed (J–L). e-spt, early spermatids; m-spt, middle spermatids; sp, mature sperm.

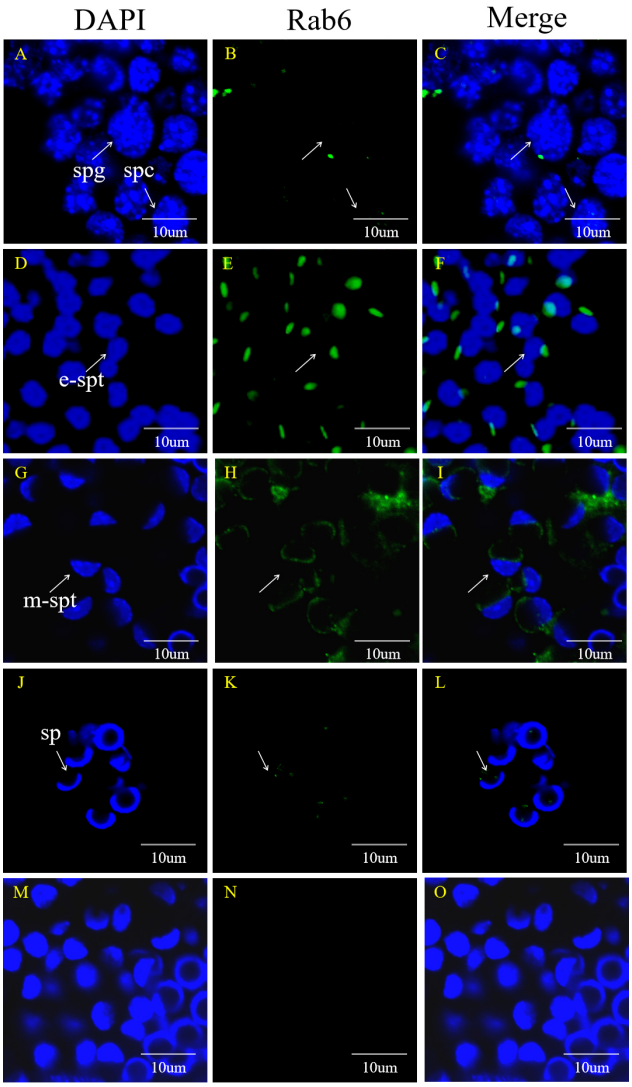


**Fig. 9. Rab6 (green) characteristics during spermatogenesis in *E.sinensis*.** Rab6 was located at one side near the nuclei in the spermatogonia and spermatocytes (A–C). In the early spermatids, the Rab6 signals were more obvious and gathered near the nuclei, indicating that they were involved in the formation of pre-acrosomal vacuoles (D–F). The signals transferred to the pre-acrosomal membrane in the middle spermatids (G–I) and finally settled on the acrosomal membrane and acrosomal tubule in the mature sperm (J–L). In the negative control, no positive signals were observed (M–O). spg, spermatogonia; spc, spermatocytes, e-spt, early spermatids, m-spt, middle spermatids, sp, mature sperm. The scale bar represents 10 μm.

membrane, indicating the involvement of Rab6 in forming subacrosomal structures. Our results showed that Rab2 and Rab6 are conserved during acrosome formation across species.

Our findings provide a foundation for studying the functions of Rab proteins in acrosome formation during spermatogenesis in Decapoda animals. This work extends our understanding of the sperm proteome in crustaceans. Further research is needed to clarify the functions of other Rab proteins that participatr in spermatogenesis and fertilization in *E.sinensis*.

## 5. Conclusions

In summary, the findings in the present research showed that a total of 1247 kinds proteins, including 7 Rab proteins, were identified in the sperm proteome in *E.sinenesis*. Ployantibodies of Rab2 and Rab6 were prepared and the the characteristics of the target Rab proteins were illustrated using IF, we found Rab2 and Rab6, though in different patterns, are involved in the acrosome formation during spermatogenesis in *E.sinensis*. The results showed that Rab proteins are key members of the acrosomal proteins and these findings provide a foundation for further illustrating the functions of Rab proteins during spermatogenesis in Decapoda animals.

## Availability of Data and Materials

The datasets used and/or analyzed during the current study are available from the corresponding author on reasonable request.

## Author Contributions

The experiments were designed by XK, JC and CL. CL, SM, and YL performed the proteome and the bioinformatics analysis; JC and HZ conducted the RNA extraction, sequencing and polyantibodies preparation. CL, JC, ZZ and MG conducted the western blot and immunofluorescence; CL and JC wrote the manuscript with essential contributions from XK. All authors revised and approved the final manuscript.

## Ethics Approval and Consent to Participate

All operating procedures and handling methods involving experimental mice were performed in accordance with the 'Guiding Opinions on the Treatment of Laboratory Animals' issued by the Ministry of Science and Technology of the People's Republic of China and approved by the Animal Ethics and Care Committee of Hebei University (approval no.: IACUC-2017013).


## Acknowledgment

Many thanks to the Instruments Sharing Platform of the School of Life Sciences of Hebei University for providing equipment support. We also thank the Jingjie company for LC-MS/MS analysis.

## Funding

This work was supported by grants from the National Natural Science Foundation of China (31572269).


## Conflict of Interest

The authors declare no conflict of interest.

## Supplementary Material

Supplementary material associated with this article can be found, in the online version, at https://doi.org/10.31083/j.fbl2808160.

## References


[1] Leiva NL, Nolly MB, Ávila Maniero M, Losinno AD, Damiani MT. Rab Proteins: Insights into Intracellular Trafficking in Endometrium. Reproductive Sciences. 2021; 28: 12–22.

[2] Bellucci A, Longhena F, Spillantini MG. The Role of Rab Proteins in Parkinson's Disease Synaptopathy. Biomedicines. 2022; 10: 1941.

[3] Liu J, Zheng X, Wu X. The Rab GTPase in the heart: Pivotal roles in development and disease. Life Sciences. 2022; 306: 120806.

[4] Margiotta A. Membrane Fusion and SNAREs: Interaction with Ras Proteins. International Journal of Molecular Sciences. 2022; 23: 8067.

[5] Langemeyer L, Fröhlich F, Ungermann C. Rab GTPase Function in Endosome and Lysosome Biogenesis. Trends in Cell Biology. 2018; 28: 957–970.

[6] Goud B, Liu S, Storrie B. Rab proteins as major determinants of the Golgi complex structure. Small GTPases. 2018; 9: 66–75.

[7] Shan MM, Sun SC. The multiple roles of RAB GTPases in female and male meiosis. Human Reproduction Update. 2021; 27: 1013–1029.

[8] Mountjoy JR, Xu W, McLeod D, Hyndman D, Oko R. RAB2A: a major subacrosomal protein of bovine spermatozoa implicated in acrosomal biogenesis. Biology of Reproduction. 2008; 79: 223–232.

[9] Iida H, Yoshinaga Y, Tanaka S, Toshimori K, Mori T. Identification of Rab3A GTPase as an acrosome-associated small GTP-binding protein in rat sperm. Developmental Biology. 1999; 211: 144–155.

[10] Djeddi A, Al Rawi S, Deuve JL, Perrois C, Liu YY, Russeau M, *et al*. Sperm-inherited organelle clearance in C. elegans relies on LC3-dependent autophagosome targeting to the pericentrosomal area. Development. 2015; 142: 1705–1716.

[11] Da Costa R, Bordessoules M, Guilleman M, Carmignac V, Lhussiez V, Courot H, *et al*. Vps13b is required for acrosome biogenesis through functions in Golgi dynamic and membrane trafficking. Cellular and Molecular Life Sciences. 2020; 77: 511–529.

[12] Morohoshi A, Miyata H, Oyama Y, Oura S, Noda T, Ikawa M. FAM71F1 binds to RAB2A and RAB2B and is essential for acrosome formation and male fertility in mice. Development. 2021; 148: dev199644.

[13] Bustos MA, Lucchesi O, Ruete MC, Tomes CN. Membrane-permeable Rab27A is a regulator of the acrosome reaction: Role of geranylgeranylation and guanine nucleotides. Cellular Signalling. 2018; 44: 72–81.

[14] Han Y, Li S, Ge L. Biogenesis of autophagosomes from the ERGIC membrane system. Journal of Genetics and Genomics. 2023; 50: 3–6.

[15] Dickson LJ, Liu S, Storrie B. Rab6 is required for rapid, cisternal-specific, intra-Golgi cargo transport. Scientific Reports. 2020; 10: 16604.

[16] Martinez O, Schmidt A, Salaméro J, Hoflack B, Roa M, Goud B. The small GTP-binding protein rab6 functions in intra-Golgi transport. The Journal of Cell Biology. 1994; 127: 1575–1588.

[17] Goud B, Zahraoui A, Tavitian A, Saraste J. Small GTP-binding protein associated with Golgi cisternae. Nature. 1990; 345: 553–556.

[18] Foster JA, Gerton GL. The Acrosomal Matrix. Advances in Anatomy, Embryology, and Cell Biology. 2016; 220: 15–33.

[19] Bae JW, Kim SH, Kim DH, Ha JJ, Yi JK, Hwang S, *et al*. Ras-related proteins (Rab) are key proteins related to male fertility following a unique activation mechanism. Reproductive Biology. 2019; 19: 356–362.

[20] Lo JCY, Jamsai D, O'Connor AE, Borg C, Clark BJ, Whisstock JC, *et al*. RAB-like 2 has an essential role in male fertility, sperm intra-flagellar transport, and tail assembly. PLoS Genetics. 2012; 8: e1002969.

[21] Solinger JA, Rashid HO, Prescianotto-Baschong C, Spang A. FERARI is required for Rab11-dependent endocytic recycling. Nature Cell Biology. 2020; 22: 213–224.

[22] Morgan NE, Cutrona MB, Simpson JC. Multitasking Rab Proteins in Autophagy and Membrane Trafficking: A Focus on Rab33b. International Journal of Molecular Sciences. 2019; 20: 3916.

[23] Guillén-Samander A, Bian X, De Camilli P. PDZD8 mediates a Rab7-dependent interaction of the ER with late endosomes and lysosomes. Proceedings of the National Academy of Sciences of the United States of America. 2019; 116: 22619–22623.

[24] Agarwal A, Panner Selvam MK, Baskaran S. Proteomic Analyses of Human Sperm Cells: Understanding the Role of Proteins and Molecular Pathways Affecting Male Reproductive Health. International Journal of Molecular Sciences. 2020; 21: 1621.
[25] Chauvin T, Xie F, Liu T, Nicora CD, Yang F, Camp DG, 2nd, *et al*. A systematic analysis of a deep mouse epididymal sperm proteome. Biology of Reproduction. 2012; 87: 141.
[26] Baker MA, Hetherington L, Reeves G, Müller J, Aitken RJ. The rat sperm proteome characterized via IPG strip prefractionation and LC-MS/MS identification. Proteomics. 2008; 8: 2312–2321.
[27] Fuentes-Albero MC, González-Brusi L, Cots P, Luongo C, Abril-Sánchez S, Ros-Santaella JL, *et al*. Protein Identification of Spermatozoa and Seminal Plasma in Bottlenose Dolphin (*Tursiops truncatus*). Frontiers in Cell and Developmental Biology. 2021; 9: 673961.
[28] Yang Y, Wang T, Yang S, Wu X, Huang W, Fan B, *et al*. Corrigendum: The Effects of Storage in vitro on Functions, Transcriptome, Proteome, and Oxidation Resistance of Giant Grouper Sperm. Frontiers in Marine Science. 2021; 8: 780244.
[29] Dietrich MA, Arnold GJ, Fröhlich T, Ciereszko A. In-depth proteomic analysis of carp (Cyprinus carpio L) spermatozoa. Comparative Biochemistry and Physiology. Part D, Genomics & Proteomics. 2014; 12: 10–15.
[30] Du N S, Xue L Z, Lai W. Studies on the sperm of Chinese mitten-handed crab, Eriocheir sinensis (Crustacea, Decapoda). II. Spermatogenesis. Oceanol Limnol Sin. 1988; 19: 71–75.
[31] Wu JL, Kang XJ, Guo MS, Mu SM, Zhang ZH. Cloning and Functional Analysis of Histones H3 and H4 in Nuclear Shaping during Spermatogenesis of the Chinese Mitten Crab, Eriocheir sinensis. PLoS ONE. 2015; 10: e0126623.
[32] Wu J, Mu S, Guo M, Chen T, Zhang Z, Li Z, *et al*. Histone H2B gene cloning, with implication for its function during nuclear shaping in the Chinese mitten crab, Eriocheir sinensis. Gene. 2016; 575: 276–284.
[33] Zhang ZH, Mu SM, Guo MS, Wu JL, Li YQ, Zhang H, *et al*. Dynamics of histone H2A, H4 and HS1ph during spermatogenesis with a focus on chromatin condensation and maturity of spermatozoa. Scientific Reports. 2016; 6: 25089.
[34] Chen T, Mu S, Sun Z, Zhang H, Li C, Guo M, *et al*. Spermiogenic histone transitions and chromatin decondensation in Decapoda. Theriogenology. 2020; 156: 242–252.
[35] Pérez-Patiño C, Parrilla I, Li J, Barranco I, Martínez EA, Rodriguez-Martínez H, *et al*. The Proteome of Pig Spermatozoa Is Remodeled During Ejaculation*[S]. Molecular & Cellular Proteomics. 2019; 18: 41–50.
[36] D'Amours O, Calvo É, Bourassa S, Vincent P, Blondin P, Sullivan R. Proteomic markers of low and high fertility bovine spermatozoa separated by Percoll gradient. Molecular Reproduction and Development. 2019; 86: 999–1012.
[37] Skerrett-Byrne DA, Anderson AL, Hulse L, Wass C, Dun MD, Bromfield EG, *et al*. Proteomic analysis of koala (phascolarctos cinereus) spermatozoa and prostatic bodies. Proteomics. 2021; 21: e2100067.
[38] Wang G, Guo Y, Zhou T, Shi X, Yu J, Yang Y, *et al*. In-depth proteomic analysis of the human sperm reveals complex protein compositions. Journal of Proteomics. 2013; 79: 114–122.
[39] Tsai YL, Lai TH, Liu HC, Wang YY, Lin YH, Ke CC, *et al*. Localization Patterns of RAB3C Are Associated with Murine and Human Sperm Formation. Medicina. 2022; 58: 1408.
[40] Bae JW, Yi JK, Jeong EJ, Lee WJ, Hwang JM, Kim DH, *et al*. Ras-related proteins (Rab) play significant roles in sperm motility and capacitation status. Reproductive Biology. 2022; 22: 100617.
[41] Rahman MS, Kwon WS, Pang MG. Prediction of male fertility using capacitation-associated proteins in spermatozoa. Molecular Reproduction and Development. 2017; 84: 749–759.
[42] Oko R, Sutovsky P. Biogenesis of sperm perinuclear theca and its role in sperm functional competence and fertilization. Journal of Reproductive Immunology. 2009; 83: 2–7.
[43] Yue X, Tiwari N, Zhu L, Ngo HDT, Lim JM, Gim B, *et al*. Tankyrase-1-mediated degradation of Golgin45 regulates glycosyltransferase trafficking and protein glycosylation in Rab2-GTP-dependent manner. Communications Biology. 2021; 4: 1370.
[44] Ding X, Jiang X, Tian R, Zhao P, Li L, Wang X, *et al*. RAB2 regulates the formation of autophagosome and autolysosome in mammalian cells. Autophagy. 2019; 15: 1774–1786.
[45] Lőrincz P, Tóth S, Benkő P, Lakatos Z, Boda A, Glatz G, *et al*. Rab2 promotes autophagic and endocytic lysosomal degradation. The Journal of Cell Biology. 2017; 216: 1937–1947.
[46] Shomron O, Hirschberg K, Burakov A, Kamentseva R, Kornilova E, Nadezhdina E, *et al*. Positioning of endoplasmic reticulum exit sites around the Golgi depends on BicaudalD2 and Rab6 activity. Traffic. 2021; 22: 64–77.